CONCRETE LIBRARY OF JSCE NO. 25, JUNE 1995

EVALUATION OF SHEAR STRENGTH OF RC BEAM SECTION BASED ON EXTENDED MODIFIED COMPRESSION FIELD THEORY

(Translation from Proceedings of JSCE, No.490/V-23, 1994)

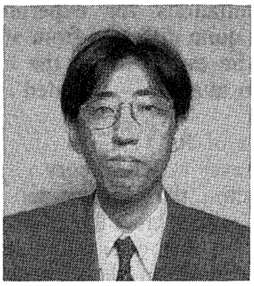

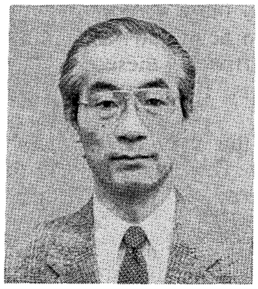

Hikaru NAKAMURA　　　Takeshi HIGAI

An analytical method to evaluate the diagonal shear failure strength of RC beams was developed, in which the modified compression field theory was extended. The effects on shear strength of effective depth, longitudinal reinforcement ratio, stiffness of longitudinal reinforcement, and concrete strength were investigated analytically. Using a proposed tension softening relation, the size effect on the shear strength can be evaluated satisfactorily by this analysis method.

Keywords: modified compression field theory, shear failure, tension stiffening effect, size effect

---

Hikaru Nakamura is an associate professor in the Department of Civil and Environmental Engineering at Yamanashi University, Kofu, Japan. He received his Doctor of Engineering Degree from Nagoya University in 1992. His research interests include failure mechanism of RC structures and application of finite element analysis. He is a member of JSCE and JCI.

Takeshi Higai is a professor in the Department of Civil and Environmental Engineering at Yamanashi University, Kofu, Japan. He received his Doctor of Engineering Degree in 1972 from University of Tokyo. His research interests relate to the shear failure of reinforced concrete structures, dynamic behavior of concrete structures and maintenance and strengthening existing concrete structures. He is a member of JSCE and JCI.

---

1. INTRODUCTION

The shear failure of reinforced concrete structures is a complicated phenomenon influenced by many factors. It appears that a full understanding of the mechanism of shear failure is extremely difficult. Given the difficulties, studies of shear have been aimed at obtaining load carrying capacity, and many studies have been based on empirical methods using many experimental results or based on limit analysis using a simple assumption of the failure mechanism.

Recently, concrete structures have become larger and more complex, and newly developed materials such as fiber reinforced plastic(FRP) have been used in concrete structures. In attempting to predict the shear strength of such structures, evaluations based on empirical methods are not necessarily effective. For example, the shear strength of RC beams has been found to gradually fall as the beam depth increases. However, it is difficult to accurately estimate the shear strength of such large RC structures because of limitations for experimental conditions. Furthermore, when new materials with material properties quite different from steel, such as FRP, are applied, the effect of these different properties must be evaluated on the basis of numerous experimental results. Thus the equation to account for them must be formulated again.

On the contrary, the study to evaluate the shear strength of RC beam analytically are recently performed activity. One such study is the modified compression field theory proposed by Collins et al.[1]. Their theory gives an analytical method for predicting the shear response of RC elements satisfying conditions of compatibility and equilibrium, in which cracked concrete is treated as a new material with its own stress-strain characteristics. The method is applicable to reinforced concrete elements in plane stress conditions and under uniform deformation. Therefore, the method does not apply to the analysis of RC beams subjected to shear, moment and axial loading.

The purpose of this paper is to analytically evaluate the shear strength of RC beam section without stirrups using an analytical method in which the modified compression field theory is extended to cover analysis of RC beams loaded with combined shear, moment and axial loading. Firstly, the analytical method is verified by comparing with an empirical method. The effects on shear strength of several factors are then investigated analytically. In particular, the effect of stiffness of the longitudinal reinforcement and the size effect are evaluated analytically in this paper.

2. ANALYTICAL METHOD BASED ON EXTENDED MODIFIED COMPRESSION FIELD THEORY

The modified compression field theory is a new analytical method for reinforced concrete elements subjected to shear developed by Vecchio and Collins[1]. The theory, however, is applicable only to elements subjected to uniform shear, and cannot be applied directly to reinforced concrete beams subjected to shear and moment loading.

In this paper, an analytical evaluation of the shear strength of RC beams is performed by extending the modified compression field theory. This is achieved by considering the cross section to be composed of a series of layers. The concept of this analytical method is similar to Collins's method[4]. However, the use of a fast computation algorithm and a tension softening curve well suited the analysis of RC beams differentiate our approach.

(1) Modified Compression Field Theory

Consider a uniform cracked reinforced concrete element subjected to uniform shear and axial loading as shown in Fig.-1. Then consider the following average strains: strain in the longitudinal direction(ε_x), strain in the transverse direction(ε_y) and shear strain(γ_{xy}) or the principal compressive strain(ε_2), principal tensile strain(ε_1) and the angle of inclination of principal compressive strain(θ). The compatibility conditions in terms of average strain in such an element are written as follows from Mohr's strain circle in Fig.-2.

$$\gamma_{xy} = 2(\varepsilon_1 - \varepsilon_x)\tan\theta \tag{1}$$

$$\varepsilon_y = \varepsilon_1 - (\varepsilon_1 - \varepsilon_x)\tan^2\theta \tag{2}$$

$$\varepsilon_2 = \varepsilon_x - (\varepsilon_1 - \varepsilon_x)\tan^2\theta \tag{3}$$

Assume that a shear stress(τ_{xy}) and a longitudinal stress(σ_x) are acting on the concrete element and that all of the shear stress is carried in the concrete. Then, the average stress relations are represented as follows from Mohr's stress circle in Fig.-3.

$$\sigma_x = \sigma_1 - \tau_{xy} / \tan\theta' \tag{4}$$

$$\sigma_y = \sigma_1 - \tau_{xy}\tan\theta' \tag{5}$$

$$\sigma_2 = \sigma_1 - \tau_{xy}(\tan\theta' + 1/\tan\theta') \tag{6}$$

in which σ_x is the longitudinal stress, σ_y is the transverse stress, τ_{xy} is the shear stress, σ_1 is the principal tensile stress and σ_2 is the principal compressive stress which has the inclination of θ'. The inclination of the principal compressive stress coincides with that of the principal compressive strain, $\theta=\theta'$, if we ignore shear transfer at the concrete crack surface.

For equilibrium in the longitudinal direction,

$$N = A_{sx}f_{sx} + \sigma_x B_w h \tag{7}$$

in which N is the applied axial force, A_{sx} is the area of the longitudinal steel bar, f_{sx} is the stress of the longitudinal steel bar, B_w is the width of the concrete element, and h is the height of the concrete element.

The equilibrium condition in the transverse direction is as follows, assuming that the transverse force does not act on the cross section.

$$\sigma_y = -A_w f_{sy} / B_w S \tag{8}$$

in which A_w is the area of the transverse steel bar, f_{sy} is the stress of the transverse steel bar, and S is the spacing between transverse steel bars. The stress of the transverse steel bar vanishes when a cross section without stirrups is considered.

The equilibrium condition in shear is

$$\tau_{xy} = V / B_w h \tag{9}$$

where V is the shear force acting on the cross section.

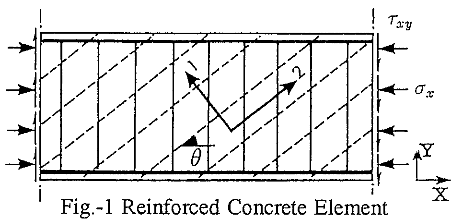

Fig.-1 Reinforced Concrete Element

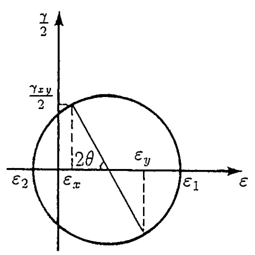

Fig.-2 Mohr's Strain Circle

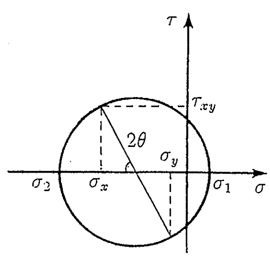

Fig.-3 Mohr's Stress Circle

The stress and strain satisfying the strain compatibility condition and the equilibrium of stresses is obtained when constitutive relations for the concrete in the principal direction and for the longitudinal and transverse steel bars are assumed, and the stresses obtained from the equilibrium condition are identical to the stresses obtained from the assumed constitutive relations. This method, however, requires a trial and error solution technique, since a direct solution cannot be obtained.

(2) Application of Modified Compression Field Theory to RC Beam Sections subjected to Axial, Moment and Shear Forces

An outline of the new analytical method is given here. The stress-strain relationship for the concrete and steel bars, then, is already available from the mechanical properties of the materials.
① Subdivide the cross section into m layers and give geometrical conditions for each layer(Fig.-4(b)).
② Give the axial force(N) and shear force(V) acting on the cross section. Here, it is assumed that the shear stress(τ_{xy}) is distributed the uniformly in the cross section(Fig.-4(d)).
③ Assume a longitudinal strain. The strain in each of the layers is fixed by defining the curvature and top strain(ε_c) in the section, assuming the distribution of longitudinal strain is linear(Fig.-4(c)).

$$\varepsilon_{xi} = (h - y_{ci})\phi + \varepsilon_c \tag{10}$$

This assumption of longitudinal strain and shear stress distribution is somewhat simplified. Thus, a more detailed investigation will be needed in future.
④ Satisfy the condition of compatibility and equilibrium for the known τ_{xy} and ε_{xi} in each layer. The following procedure is performed in each layer:

(a) Assume the principal tensile strain(ε_1).
(b) Calculate the principal tensile stress(σ_1) corresponding to ε_1 using the concrete stress-strain relationship.
(c) Calculate θ from the equilibrium in the transverse direction.
From the transverse equilibrium, the stress of a transverse steel bar is

$$f_{sy} = -B_w S / A_w(\sigma_1 - \tau_{xy} \tan\theta) \tag{11}$$

On the other hand, the stress of a transverse steel bar obtained from the compatibility condition and stress-strain relationship of transverse steel is

$$f'_{sy} = E_{sy}\left\{\varepsilon_1 - (\varepsilon_1 - \varepsilon_x)\tan^2\theta\right\} \tag{12}$$

Considering the condition $f_{sy}=f'_{sy}$ using Eq(11) and Eq(12), we obtain a quadratic equation in $\tan\theta$ before the steel bar yields or a linear equation after yielding. From the algebraic equations of $\tan\theta$, we can identify θ positively.
(d) Calculate the principal compressive strain(ε_2), the transverse strain(ε_y), and the shear strain (γ_{xy}) from the Mohr's strain circle.
(e) Calculate the longitudinal stress(σ_x), transverse stress(σ_y), and the principal compressive stress (σ_2) from Mohr's stress circle.
(f) Calculate σ'_2 from ε_2 using the concrete stress-strain relationship.
(g) If σ_2 does not equal σ'_2, return to step (a) and try another value of ε_1.

⑤ Repeat (a) to (g) until the equilibrium and compatibility conditions are satisfied for all layers.
⑥ Calculate the stress of longitudinal steel bar(f_{sxi}) from the longitudinal strain of the steel bar.

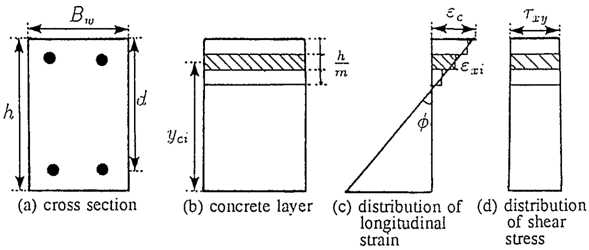

Fig.-4 Beam Section using Layered Model

⑦ Calculate the resultant of the longitudinal stresses. Also check the equilibrium of applied axial force. If the equilibrium conditions are not satisfied, it is necessary to readjust the assumed ε_c and repeat the analysis until equilibrium is satisfied.
⑧ Calculate the moment acting on the section from the distribution of longitudinal stresses.

Using the above procedure, the moment acting on the section is calculated for the applied axial and shear force. To obtain the equilibrium condition for the moment, a convergence calculation of curvature is needed. The solution algorithm used by Collins et al. involves the convergence process of ε_2 and θ for each layer, and that of the longitudinal strain distribution for the cross section. On the other hand, procedure described here has only one convergence process for ε_1 in each layer and ε_c for the cross section. Therefore, computational analysis is fast using few unknowns to reach convergence.

The ultimate states are defined in the analysis by the following two cases when curvature is increased under the condition of constant axial and shear force.
(1) The maximum compressive strain in the cross section is reached at the strain corresponding to the strength of the concrete(-0.002).
(2) No solution satisfying the equilibrium for the given ε_x and τ_{xy} is obtained in at least one layer, even if the equilibrium condition for axial force is satisfied.

Therefore, the ultimate loading capacity is obtained from the moment corresponding to each cases. The failure modes are thus distinguished between flexural failure for case(1) and shear failure for case(2). Using the above definition, it is possible to define the ultimate loading capacity depending on the different failure mode in the analysis.

(3) Material Modeling

a) Concrete

The stress-strain relationship for the concrete used is shown in Fig.-5. In the zone of compression, the relationship is represented by a second degree parabola up to the maximum compressive stress. The maximum compressive stress decreases depending on the principal tensile strain ε_1 using an equation proposed by Collins et al.[3]. However, Miyahara et al.[5] reported that the maximum compressive stress becomes constant value for higher tensile strains in cracked concrete. Thus, it is assumed in the analysis that the maximum compressive stress becomes constant when the principal tensile strain exceeds 40 times the crack strain. The stress-strain relationship beyond the compressive strength is not considered since the object of this analysis is shear failure.

In the tension zone, the stress increases linearly with a constant proportionality of $2f'_c/\varepsilon_{co}$ up to the tensile strength(f_t). After that, it is evaluated by the following equation which modifies the equation proposed by Collins et al.[3].

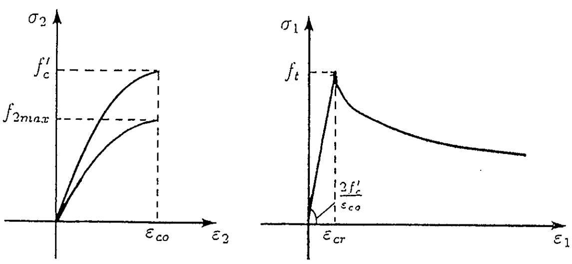

Fig.-5 Stress-Strain Relation of Concrete

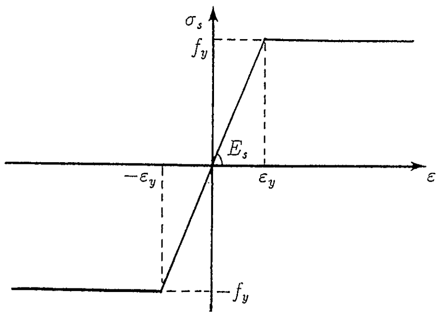

Fig.-6 Stress-Strain Relation of Reinforcement

$$\sigma_1 = \frac{f_t}{1+\alpha\sqrt{200(\varepsilon_1-\varepsilon_{cr})}} \tag{13}$$

This equation modifies the stress reduction by introducing the coefficient α into the Collins equation. The concept of coefficient α and the equation is based on the following discussion. Equation(13) is the relation between average tensile stress to average tensile strain in a cracked reinforced concrete element. The Collins equation, however, was formulated from experimental result for RC membrane elements arranged with a reinforcement mesh having equi-grid spacing. Thus, we predicted that it is not applicable to RC beams with the reinforcement arranged concentrically to the lower part of the cross section. Moreover, it is guessed that the bonding effect between concrete and steel which dominates this relation operates over a specific area around the steel bar. However, it must be assumed that the effect influences all tensile area of the cross section in the analysis, because the area has not been clarified at present. The correction to the area influenced by the bonding effect is accomplished by coefficient α. This is the feature in this study that the stress-strain relationship in tensile, that is tension softening curve, is varied by coefficient α.

b) Reinforcement

The stress-strain relationship for the reinforcement is shown in Fig.-6. It is assumed that the stress is proportional to the strain with the initial stiffness up to the yielding point, and that the yield stress remains constant after that in both tension and compression zones.

3. INVESTIGATION OF APPLICABILITY OF EXTENDED MODIFIED COMPRESSION FIELD THEORY

(1) Effect of Tension Softening Behavior

As mentioned above, it seems that analysis using the tension softening curve proposed by Collins et al. overestimates the shear strength of RC beams. We therefore estimate the value of α so as to define a tension softening curve suitable for RC beams.

The model used in this analysis is a cross section of 20 × 20cm and a beam depth of 16cm as shown in Fig.-7. The material properties are that compressive strength of concrete is 280kgf/cm ^{2}, tensile strength of concrete is 28kgf/cm ^{2}, the yielding stress of the reinforcement is 3780 kgf/cm ^{2} and the initial stiffness of the reinforcement is 1.7 × 10 ^{6} kgf/cm ^{2}. The cross section is subdivided into 20 layers and the applied axial force is zero in the analysis.

The relationships between shear strength and shear span ratio(a/d) are illustrated in Fig.-8, in which α takes the values 1,3, and 5. The analytical results for α=1 are shown with mark " ● ", that of α=3 are shown with mark" △ " and that of α=5 are shown with mark " ■ ". The marks in the figure are obtained according to the definition of failure mentioned above. Then, the values of a/d are calculated supposing a=M/V for two-point loading and a simply supported beam. As a result, the failure section in the beam is defined in the maximum moment section. In the figure, the broken line indicates the moment capacity curve and the solid line indicates the shear strength curve obtained from the equation proposed by Niwa et al.(Eq(14))[6]. The applicability of the analysis of shear strength is investigated by comparison with Niwa's equation, supposing that this equation gives the correct solution for diagonal tension failure strength since it was formulated from many experimental data and its reliability is already proven. It should be noted that the following analysis is restricted to RC rectangular sections.

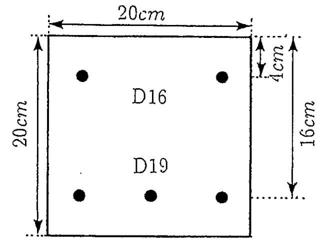

Fig.-7 Analytical Model

$$V = 0.94 f_c'^{1/3} (100 P_w)^{1/3} (d/100)^{-1/4} (0.75 + 1.4 d/a) B_w d \tag{14}$$

in which f'_c is the compressive strength of concrete, P_w is the longitudinal reinforcement ratio, d is the effective depth of the cross section, a/d is the shear span ratio and B_w is the width of the cross section.

As shown in Fig.-8, the results for α=1, which the Collins equation is used, overestimate the shear strength and results with α=5 underestimate it. On the other hand, results with α=3 show good agreement with Eq.(14) in the range of diagonal tension failure a/d>3.

$$\sigma_1 = \frac{f_t}{1 + 3\sqrt{200(\varepsilon_1 - \varepsilon_{cr})}} \tag{15}$$

Analytical results are in good agreement with the moment capacity curve in the range of a/d>6. They are also in good agreement with the shear failure curve in the range of 3<a/d<6. It is therefore clear that this analysis can calculate both shear and flexure failure strength when the shear span ratio is varied, as long as the tension softening curve in Eq.(15) is applied. Further, the analytical results for both ranges correspond to the definition of the failure mode as mentioned above. However, the strength is underestimated when a/d is less than 3. This is the reason for the shear strength increasing as a/d becomes smaller by the effect of support and loading point; that is, the effect of compressive stress in the transverse direction. However the analysis does not consider this effect. Consequently, this analysis can evaluate the flexure and diagonal tension failure strength, but it will be necessary for the shear compression failure strength to be investigated in more detail.

Many tension softening curves have been proposed. The curve proposed here is similar to that proposed by Okamura and Maekawa[7] for deformed steel bars, as shown in Fig.-9. Therefore, it is guessed that the proposed curve is adequate for RC beams. However, further modification of the curve for effective depth is investigated in next section, since the averaging bonding effect between concrete and reinforcement is influenced by the effective depth.

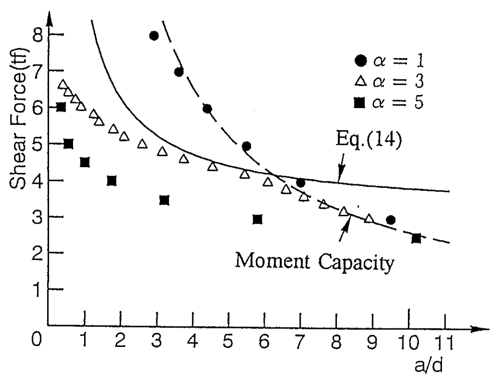

Fig.-8 Effect of Tension Softening Curve

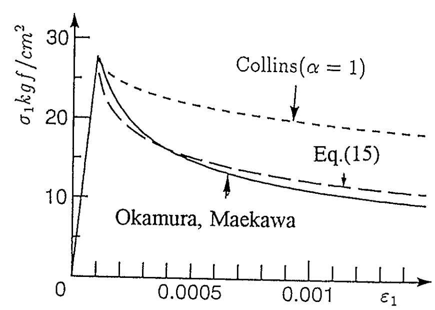

Fig.-9 Comparison of Tension Softening Curves

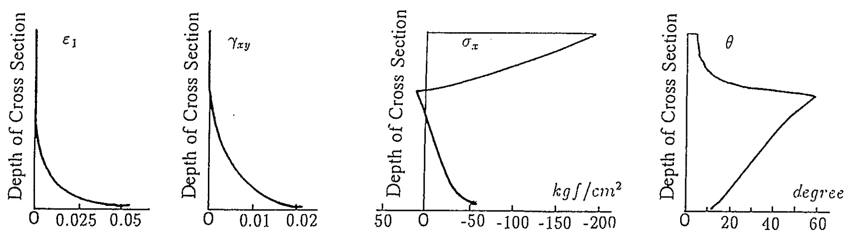

Fig.-10 Distribution of Stress, Strain, and Angle

Figure-10 shows the analytical results of the distribution of strain, stress, and angle of inclination of principal compressive strain just before failure(N=0tf, V=5000tf, M=2.08 $\times$ 10 ^{5} tf·m). The principal tensile strain and shear strain increase rapidly near the lower part of the cross section, and the longitudinal stress becomes compression due to the effect of the bi-axial stress field in the lower part.

(2) Effect of Subdivided Layer Number

It is predicted that the results of analysis will be influenced by the number of subdivided layers. Thus, the effect of subdivided layer number is investigated here. The analysis is performed for four cases, in which the cross section shown in Fig.-7 is subdivided into 40, 20, 10 and 5 layers. Figure-11 shows the relationships between shear force and moment obtained in this analysis. The results for 5, 10, 20 and 40 layers are marked with " ○ ", " △ ", " □ " and " × ", respectively. It is clear that the results converge when number of layers is more than 20 layers. Therefore, we adopt 20 layers in the following analysis.

4. EFFECTS ON SHEAR FAILURE STRENGTH OF RC BEAM SECTION WITHOUT STIRRUPS OF VARIABLE FACTORS

We investigate the effects of variable factors on shear strength in this section. The model used in this analysis is the RC cross section shown in Fig.-7. The analytical results are verified by comparison with Niwa's equation, which was formulated on the basis of many experimental results.

(1) Effects of Effective Depth

The analysis in which effective depth was varied was performed under the condition that the longitudinal reinforcement ratio is constant(P_w=0.0269). The shear strength obtained from the analysis for several effective depths is shown in Fig.-12, when M/(Vd)=3.0. The marks with " ● " in the figure are the results obtained by using the tension softening curve of Eq.(15) and the solid line is the value of Eq.(14). The analytical shear strength increases in proportion with effective depth increase and the difference from Eq.(14) increases as the effective depth increases. In general, the shear strength of RC beams is affected by size and Niwa's equation also incorporates this effect. On the contrary, this result shows that the analysis cannot evaluate the size effect. Figure-13 shows the distribution of σ_x and θ at failure when the effective depth is 16, 64 and 160cm. The distributions can be identified for every effective depths. This implies that the size effect does not appear in the analysis. The reason is that the tension softening curve used is the same(Eq.(15)) in spite of the different effective depth.

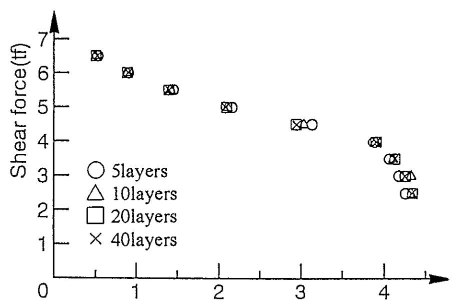

Fig.-11 Effect of Layer Number

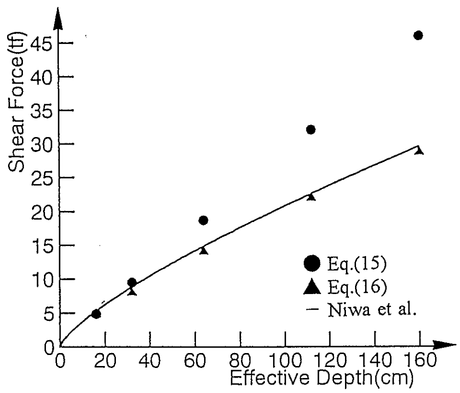

Fig.-12 Effect of Tension Softening Curve and Effective Depth on Shear Strength

Therefore, we try to estimate a tension softening curve involving the effect of size by varying the value of α in Eq.(13). The value of α will be estimated in comparison with Eq.(14) for the cross section in which effective depth is less than 160cm, because the applicability of Eq.(14) to the size effect is already appreciated experimentally within the above effective depth. Note that the tension softening curve represents the bonding effect averaged over all the cracked area.

Figure-14 shows the relationship between α and effective depth obtained in the analysis. The analytical results are marked with " ○ ", and the solid line is the following equation of relationship of α versus effective depth obtained from an interpolation of the analytical results.

$$\alpha = 3(d/16)^{1/3} \tag{16}$$

A tension softening curve involving the effect of effective depth is obtained by substituting Eq.(16) into Eq.(13). The results using the Eq.(16) are shown by " ▲ " in Fig.-12. It is clear that the size effect can be evaluated analytically using Eq.(16) in a similar to Eq.(14). Figure-15 shows the analytical results for an effective depth of 112cm. The marks with " ● " are analytical results, the broken line is the shear strength curve of Eq.(14), and the solid line is the moment capacity curve. The analytical results are good agreement with Eq.(14) over a wide range.

The physical meaning of Eq.(16) is not clear since it was obtained only from an analytical comparison with Eq.(14). Moreover, we must verify the applicability of the equation to very large cross sections which is not possible experimentally. Thus the applicability to the large-scale cross sections is investigated below using a energy consideration.

The shear strength(V_1, V_2) and the strain softening energy(W_1, W_2) obtained from analysis using Eq.(16) and Eq.(15) for d=16, 64, 160 and 1600cm are shown in Table-1. The strain softening energy is defined as the principal strain energy absorbed in the cracked concrete section up to failure. That is,

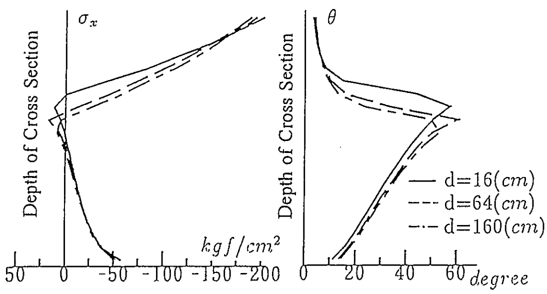

Fig.-13 Distribution of σ_x and θ using Eq.(15)

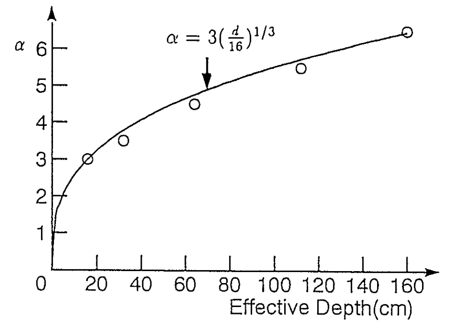

Fig.-14 Relation between Effective Depth and α

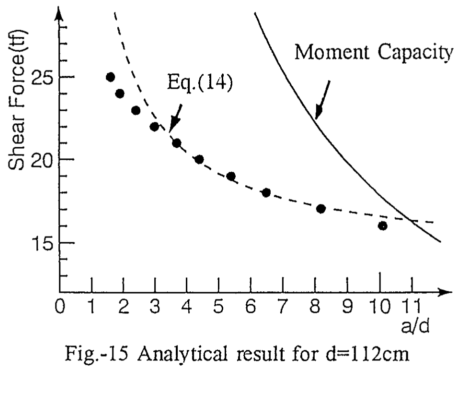

Fig.-15 Analytical result for d=112cm

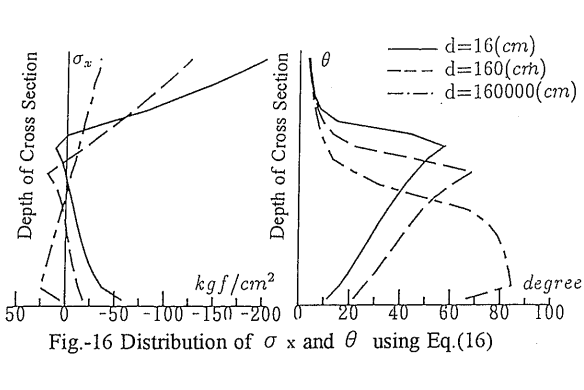

Fig.-16 Distribution of σ_x and θ using Eq.(16)

$$W = \int_{-h/2}^{h_{cr}} \int_{\varepsilon_{cr}}^{\varepsilon_1} \sigma_1(\varepsilon_1) d\varepsilon dy \tag{17}$$

It is understood that the strain softening energy(W_2) used Eq.(15) increases in proportion with effective depth increase. The results mean that the size effect does not considered obviously based on the consideration of energy in this case. On the other hand, energy(W_1) used in Eq.(16) is almost same although the effective depth is changed. That is, although energy(W_1) increases slightly with effective depth increase, the increment is about three times when the effective depth varies from 16cm to 1600cm, and the effect of effective depth on energy is negligible. This result implies that the analysis is applicable to very large cross sections on the assumption that the energy absorption is constant and independent on size at the ultimate state. Figure-16 shows the distribution of σ_x and θ at failure for different effective depths. The distributions are different from effective depth and the effect of size appear obviously.

(2) Effects of Longitudinal Reinforcement Ratio

An analysis in which the longitudinal reinforcement ratio is varied was performed for the RC cross section shown in Fig.-7. The ratio is given nine values from 0.5% to 5.0%. The relationships between shear force and moment in the failure state are illustrated in Fig.-17. Moment increase in proportion as the shear force decrease and maintain constant values(moment capacity) for smaller shear force. The range in which the moment is constant and the shear force decreases rapidly corresponds to the flexural failure region as defined in the analysis (maximum compressive strain of -0.002). On the other hand, the range in which the shear force decreases gradually corresponds to the shear failure region. As shown in the figure, the curves for each longitudinal reinforcement

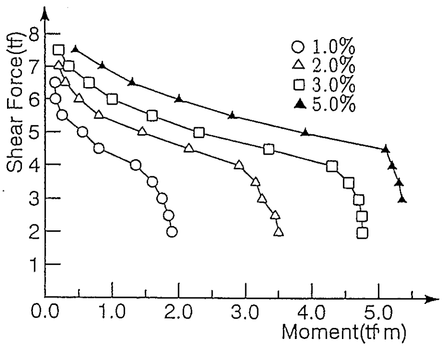

Fig.-17 Effect of Longitudinal Reinforcement

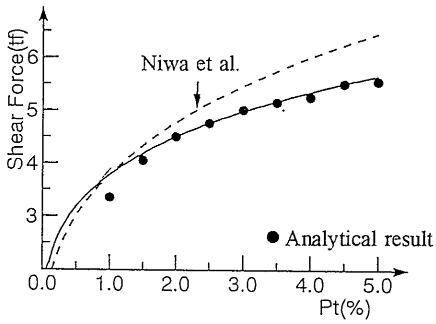

Fig.-18 Relation between Longitudinal Reinforcement Ratio and Shear Strength

Table-1 Effect of Effective Depth

Effective Depth d(cm)	Analysis Eq.(16) V_1(tf)	Analysis Eq.(15) V_2(tf)	Niwa et al. V_c(tf)	V/V_c	Strain Softening Energy W_1(kgf/cm)	Strain Softening Energy W_2(kgf/cm)
16 (0.25)	4.85	4.85 (0.26)	5.26	0.92	0.878 (0.91)	0.878 (0.44)
64 (1.0)	14.2	18.7 (1.0)	14.8	0.95	0.963 (1.0)	1.976 (1.0)
160 (2.5)	29.2	46.0 (2.46)	29.5	0.98	1.319 (1.37)	4.157 (2.1)
1600 (25.0)	181.0	460.0 (24.6)	166.2	1.09	2.555 (2.65)	39.87 (20.18)

V_1:Analytical result using Eq.(16) V_2:Analytical result using Eq.(15)
W_1:Strain softening energy corresponding to V_1
W_2:Strain softening energy corresponding to V_2
Values in parentheses are normalized to d=64cm

ratio are parallel. This implies that the effect of longitudinal reinforcement ratio on shear strength is independent of the moment and is a function of only the longitudinal reinforcement ratio.

Figure-18 shows the relationship between longitudinal reinforcement ratio and shear strength for M/(Vd)=3. The marks " ● " indicate analytical values and the broken line represents Eq.(14). The difference between the analytical values and Eq.(14) increases with increasing longitudinal reinforcement ratio. The solid line in the figure represents the shear strength obtained from the equation in which the longitudinal reinforcement ratio term in Eq.(14) is modified from $(Pw)^{1/3}$ to $(Pw)^{1/4}$. It is understood that the shear strength analyzed is proportional to $(Pw)^{1/4}$. Although the analytical result has a tendency to be different from Eq.(14), the difference is insignificant as regards applicability of the analysis, since the difference is less than 10% when the longitudinal reinforcement ratio is in the range of practical use($0.3\%<Pw<3.0\%$).

(3) Effects of Longitudinal Reinforcement Stiffness

The equations proposed for shear strength in the past do not consider the effects of longitudinal reinforcement stiffness, since the use of steel bars is a premise in the reinforcement of concrete. Recently, fiber reinforced plastic(FRP), whose stiffness is lower than that of steel bars, has been developed as a substitute for steel bars in the reinforcement of concrete. It has been reported experimentally that the shear strength of concrete beams reinforced with FRP is lower than that of beams reinforced with steel bars. Thus, we investigate the effect of the stiffness of reinforcement.

An analysis is performed in which the stiffness of the reinforcement is varied from 0.25×10^6 to 2.0×10^6 kgf/cm^2 for the RC cross section shown in Fig.-7. The results of analysis are shown in Fig.-19. It is understood that the stiffness of the reinforcement is a factor which influences shear strength. The results indicate that the shear strength is proportional to the 1/4 power of reinforcement stiffness. That is, the effect of longitudinal reinforcement stiffness is similar to the effect of longitudinal reinforcement ratio.

$$V = V_c (E_i / E_s)^{1/4} \tag{18}$$

Tsuji et al.[8] proposed a method of evaluating the shear strength of concrete beams reinforced with FRP by the transformed area of steel bar($A_s(E_i/E_s)$) considering the difference in stiffness. The results of analysis prove that this method is adequate. However, the effects of stiffness as proposed by Tsuji et al. differ from this analysis. The effect of stiffness on shear strength is represented by a 1/3 power, since Tsuji et al. use the JSCE equation.

The effect of stiffness is verified by a comparison with the experimental data presented by Tsuji et al.. Figure-20 shows the ratio of estimated and experimental values of shear strength. The

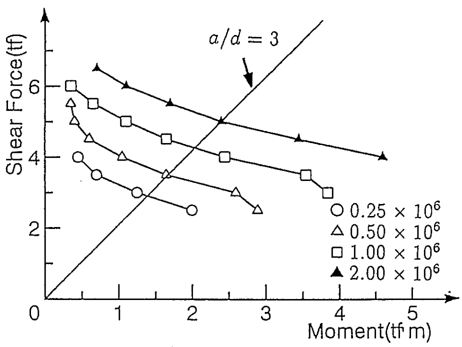

Fig.-19 Effect of stiffness of Longitudinal Reinforcement

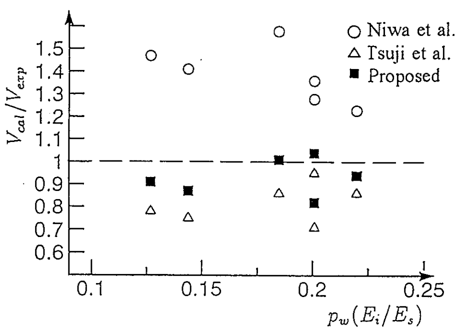

Fig.-20 Ratio of Estimated and Experimental Values

Table-2 Effect of Compressive Strength

f'_c (kgf/cm^2)	V (kgf)	$f'_c/280$	V/4850
75	4150	0.268	0.856
150	4600	0.536	0.948
280	4850	1.0	1.0
450	4950	1.61	1.021

Table-3 Effect of Tensile Strength

f_t (kgf/cm^2)	V (kgf)	$f_t/28$	V/4850
14	3000	0.5	0.618
28	4850	1.0	1.0
42	6400	1.5	1.319

estimated values are obtained from Eq.(14), the method of Tsuji et al., and Eq.(18). When the effect of stiffness is evaluated by the 1/3 power longitudinal reinforcement stiffness as proposed by Tsuji et al., the shear strength is underestimated. On the other hand, the effect of stiffness is evaluated more accurately by Eq.(18) where the effect is represented by the 1/4 power of longitudinal reinforcement stiffness.

(4) Effect of Concrete Strength

An analysis in which the compressive strength is varied was performed under the condition that the tensile strength is f_t=28kgf/cm^2. The compressive strength was set to four values from 75 to 450 kgf/cm^2. The results of the analysis are shown in Table-2 when M/(Vd)=3. Although the shear strength increases slightly with increasing f'_c, the effect does not appear clear analytically. The results imply that the compressive strength is not an important factor in shear strength. The reason for compressive strength not having clear effect in the analysis is that initial value of compressive strength is not analytically important, since the strength varies as a function of principal tensile strain in the bi-axial stress field of the analysis.

The analysis of variations in tensile strength was performed under the condition of the compressive strength of 280kgf/cm^2. Three values of tensile strength were used: 14, 28 and 42kgf/cm^2. The results of analysis are shown in Table-3 when M/(Vd)=3. The shear strength increases in proportion to tensile strength and the results show that the tensile strength is a major factor influencing shear strength. Moreover, it appears from the analysis that the shear strength increases in proportion to approximately the 2/3 power of tensile strength.

The relationship between compressive and tensile strength is prescribed as the 1/2 power by the ACI or the 2/3 power by the JSCE. Therefore, if the above relations are correct, the result obtained from the analysis that the shear strength is proportional to the 2/3 power of the tensile strength, imply that the shear strength is a function of $(f'_c)^{1/3}$ in the ACI case or a function of $(f'_c)^{4/9}$ in the JSCE case. We conclude that the effect of concrete strength obtained from the analysis is almost the same as that given by Niwa's equation.

5. CONCLUSIONS

(1) The load carrying capacity of an RC section was evaluated by analysis based on the extended modified compression field theory. Using this analytical method, both shear and flexure failure strength can be evaluated accurately.

(2) The solution algorithm adopted in this analytical method involves convergence of ε_1 for each layer and of ε_c for the cross section. This makes possible fast numerical analysis in comparison with Collins's algorithm, since the convergence parameters are few.

(3) A tension softening curve considering the effect of size was proposed. Using the proposed tension softening relationship, the size effect on shear strength can be evaluated satisfactorily. It was proven from a consideration of energy that the analysis is applicable to very large cross sections for which experiments are not feasible.

(4) The effects on the shear strength of RC beams without stirrups of effective depth, longitudinal reinforcement ratio, longitudinal reinforcement stiffness, and concrete strength were investigated analytically.

(5) The effect of longitudinal reinforcement stiffness can be represented similarly to the effect of longitudinal reinforcement ratio. Analytical results indicate that the shear strength is proportional to the 1/4 power of longitudinal reinforcement stiffness. Moreover, the shear strength of concrete beams reinforced with FRP can evaluated accurately by considering the effect of the 1/4 power of stiffness.

(6) It appears from the analysis that the shear strength increases in proportion to the 2/3 power of tensile strength and is not influenced by the compressive strength.

References

[1] Frank J. Vecchio and Michael P.Collins : The modified compression field theory for reinforced concrete elements subjected to shear, ACI Journal, March-April, pp.219-231,1986.
[2] Frank J. Vecchio and Michael P.Collins : Predicting the response of reinforced concrete beams subjected to shear using modified compression field theory, ACI Structural Journal, May-June, pp.258-268,1988.
[3] Michael P. Collins : Towards a rational theory for RC member in shear, Proc. of ASCE, ST4, pp.649-666, April,1978.
[4] Frank J. Vecchio and Michael P.Collins : The response of reinforced concrete to in-plane shear and normal stresses, Publication No.82-03, Dept. of Civil Eng., Univ. of Toronto, Mar, 1982..
[5] Miyahara T., Kawakami T. and Maekawa K. : Nonlinear behavior of cracked reinforced concrete plate element under uniaxial compression, Proc. of JSCE, No.378/V-6, pp.249-258, 1987.
[6] Niwa J., Yamada K., Yokozawa K. and Okamura H. : Revaluation of the equation for shear strength of reinforced concrete beams without web reinforcement, Proc. of JSCE, No.372/V-5, pp.167-176, 1986.
[7] Okamura H. and Maekawa K. : Non-linear finite element analysis of reinforced concrete, proc. of JSCE, No.360, pp.1-10, 1985.8.
[8] Tsuji Y., Saito H., Sekijima K. and Miyata S. : Flexural and shear behaviors of concrete beams reinforced with FRP, Proc. of JCI, No.10, pp.547-552, 1988.